

## ARTICLES

## Mechanistic Study of Excitation Energy Transfer in Dye-Doped PPV Polymers

Klemens Brunner,<sup>\*,†</sup> John A. E. H. van Haare,<sup>‡</sup> Bea M. W. Langeveld-Voss,<sup>‡</sup>  
Herman F. M. Schoo,<sup>‡</sup> Johannes W. Hofstraat,<sup>†</sup> and Addy van Dijken<sup>†</sup>

*Philips Natuurkundig Laboratorium, Prof. Holstlaan 4, 5656 AA Eindhoven, The Netherlands, and TNO Industrial Technology, De Wielen 6, 5600 HE Eindhoven, The Netherlands*

*Received: November 1, 2001; In Final Form: February 18, 2002*

The mechanism of excitation energy transfer is studied using host–guest systems consisting of green and yellow emitting poly(phenylene vinylene) (PPV) based polymers into which red emitting dyes are dispersed. The photoluminescence from such polymer–dye systems is studied in the steady-state and time resolved. Furthermore, the electroluminescence from devices containing these polymer–dye systems as emissive layer is measured. It is shown that in such disordered polymers, characterized by dispersive exciton transport, energetic resonance between the polymer and the dye is not the only requisite for efficient energy transfer. In addition, the exciton kinetics of the combined polymer–dye system has to be taken into account. Efficient transfer of excitation energy from a disordered polymer to a dye can only occur if, at a certain energy, the polymer-to-dye exciton transfer rate is higher than the intrapolymer exciton migration rate. A consequence of the mechanism described here is that when a dye is dispersed into a disordered polymer, always a residual polymer emission remains, both in photoluminescence as well as in electroluminescence, provided that excitons are created on the polymer. This knowledge is important when constructing a device employing such a polymer–dye system as the emissive layer.

## Introduction

Light-emitting diodes using conjugated polymers as the emitting material (pLEDs) have received considerable attention since they were first reported.<sup>1</sup> Much effort has been directed toward understanding and optimizing these devices. Meanwhile, monochrome pLEDs are close to becoming available as displays in commercial products, and research activities are being focused on the next-generation displays, which will be full-color. A commonly used route for making full-color pLEDs is to incorporate luminescent dopants into the polymer layer. In principle, by using doped polymers one can achieve an increase in both efficiency<sup>2</sup> and stability, and in addition a decrease in emission bandwidth and a reduced reabsorption of emitted photons. Furthermore, it is possible to tune the color by using different luminescent dopants. The ideal device would be a full-color pLED based on a single type of polymer whose emission color is determined by the presence of dopants. The concept of using dopants to tune the emission color of a polymer is well-known, and especially organic dyes have been used for this purpose.<sup>3–12</sup>

In a pLED containing a doped polymer, important processes are charge trapping and/or energy transfer. This article focuses on energy transfer from a polymer to a dopant. Generally, for energy transfer between an excited donor and an acceptor to occur at all, it is a prerequisite that the acceptor contains states that are energetically resonant with excited states of the donor.

In most publications dealing with energy transfer in doped polymers, energetic resonance is considered to be the most important parameter for efficient energy transfer. These publications ignore the important fact that the donor (i.e., a polymer) has a high intrinsic exciton mobility.<sup>13,14</sup> To account for this, in addition to the donor–acceptor exciton kinetics, the donor–donor exciton kinetics have to be considered as well. Such a superposition of donor–donor and donor–acceptor exciton kinetics is known in the literature (e.g., for molecules that are randomly distributed in space<sup>15</sup>), but in this article it is applied to the study of energy transfer in doped polymers. The rationale for this approach is that the polymers in pLEDs are highly disordered and can be considered as ensembles of chromophores, each chromophore being a subunit of a polymer chain characterized by a certain HOMO–LUMO energy separation depending on the conjugation length and the chemical surroundings of the chromophore. This ensemble of chromophores is represented by an inhomogeneously broadened density of states. The dynamics of excitons within this inhomogeneously broadened density of states is known as dispersive transport.<sup>13,16–19</sup> This means that after an exciton is created it can be transferred to a nearby chromophore, generally with a lower HOMO–LUMO energy separation. In principle, excitons can also be transferred to chromophores with a higher HOMO–LUMO energy separation if suitable thermal phonons are present. As the exciton gradually loses some of its energy by downhill relaxation through the inhomogeneously broadened density of states, the probability for a subsequent relaxation step decreases as the concentration of chromophores with a lower HOMO–LUMO energy separation decreases.

\* Corresponding author. E-mail: klemens.brunner@philips.com

<sup>†</sup> Philips Natuurkundig Laboratorium.

<sup>‡</sup> TNO Industrial Technology.

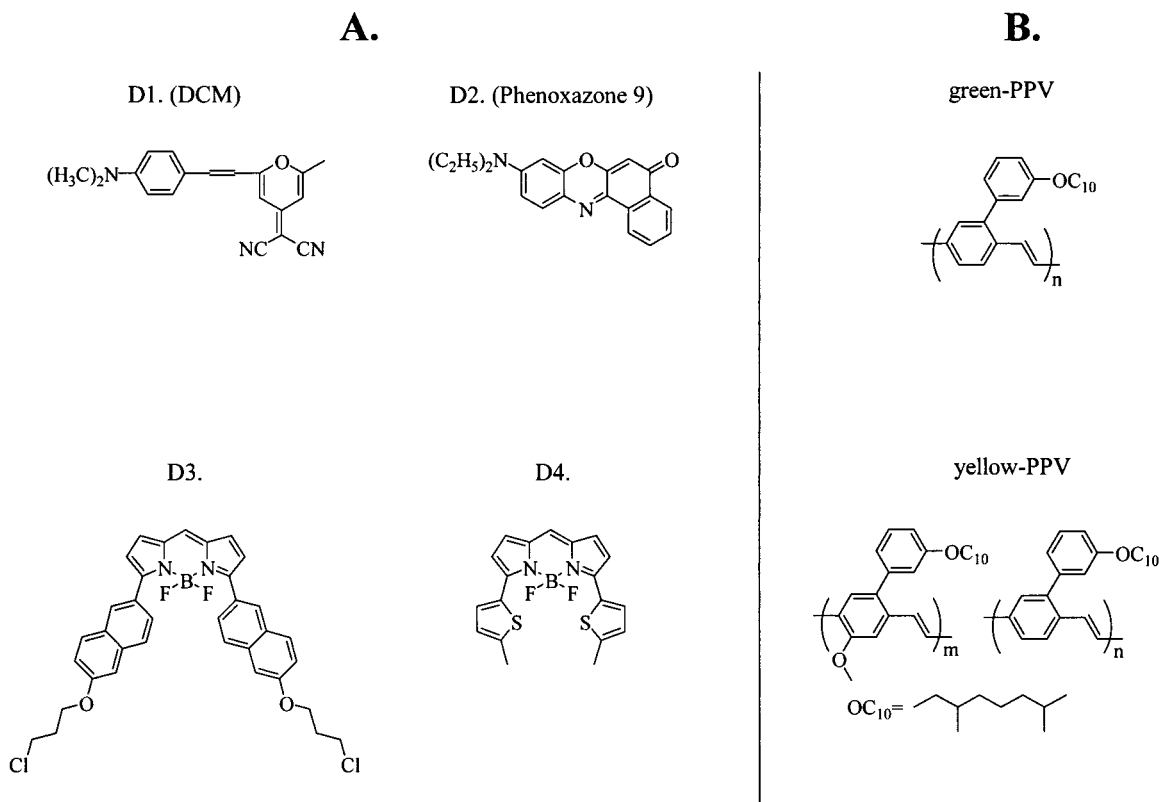


**Figure 1.** (A) Structural formulas of the dye molecules D1 (DCM), D2 (Phenoxazone 9), and the 3,5-diaryl-4,4-difluoro-4-bora-3a,4a-diaza-s-indacene based dyes D3 and D4; the maximum of the absorption band shifts to lower energy going from D1 to D4. (B) Structural formulas of the green (green-PPV) and yellow (yellow-PPV) emitting PPV-based polymers.

The systems that are described here are dispersions of dye molecules in poly(phenylene vinylene) (PPV)-based polymers, comparable to the polymers commonly used in pLEDs.<sup>20</sup> The conclusions are not specific for these systems but should be applicable to doped polymers in general. They provide important guidelines for the preparation of dye dispersions in disordered polymers that should exhibit efficient polymer-to-dye energy transfer.

### Experimental Section

**Materials.** The structures of the polymers and dyes are shown in Figure 1. Green and yellow emitting PPV-based polymers were prepared via the Gilch polymerization route<sup>21,22</sup> and will be denoted as green- and yellow-PPV respectively in the remainder of this text. The dyes D1 and D2 were obtained from Aldrich and Lambda Physik, respectively. The dyes D3 and D4 were prepared at TNO Industrial Technology. For every dye several samples with different polymer–dye mass ratios were prepared, and those exhibiting the most efficient energy transfer are presented in this article. In this way, concentration quenching was kept at a minimum. Typically, the dye was dispersed in the polymer at a mass ratio of 0.75%.

**Sample Preparation.** All samples were prepared in a glovebox under N<sub>2</sub> atmosphere. A polymer/toluene solution containing 4.5 mg/mL polymer is stirred at room temperature overnight and heated at 70 °C for 1 h before the dye is added from a stock solution in toluene (4 mg/mL). The polymer+dye/toluene solution is stirred at room temperature for 1 h and filtered over a 5 μm PTFE filter (Millex, Millipore) prior to spin coating, using a BLE Delta 20 BM spin coater. For photoluminescence measurements the emissive layer is spin coated on plain glass. For electroluminescence measurements, glass substrates patterned with a 120 nm transparent ITO layer

are used. These substrates are treated for 10 min with UV/O<sub>3</sub> (UVP PR-100) prior to any further processing. Remaining dust particles are blown away with ionized nitrogen before 150 ± 5 nm of a conductive polymer (poly(3,4-ethylenedioxythiophene), PEDOT, from Bayer AG) and 70 ± 5 nm of the emissive layer are spin coated on the substrates. The layer thickness was measured using a Dektak<sup>3</sup> ST surface profile measuring system. In these devices, the ITO/PEDOT stack serves as anode. A Ba/Al cathode is applied by vacuum evaporation using a self-built evaporation chamber.

**Measurements.** The time correlated single photon counting (TCSPC) measurements were performed on a system described elsewhere in greater detail.<sup>23</sup> The temporal resolution of the TCSPC system (90° configuration) is ~20 ps. To exclude polarization effects a magic angle detection scheme was chosen. Appropriate filters (Schott) were used to exclude scattered light. The excitation beam was not tightly focused on the polymer film, a spot size of a few mm<sup>2</sup> was enough to achieve a reasonable count rate (the excitation power was kept in the μW regime and the single photon counting limit was not exceeded). The excitation was carried out at 3.84 eV, and typical measurement times were 5–10 min, depending on the sample. The samples were prepared in a glovebox and sealed to exclude oxygen and water. Despite these precautions a slight decrease of emission intensity was observed in all cases while measuring. The steady-state photoluminescence spectra were recorded on a standard Perkin-Elmer LS 50B spectrometer using 3.02 eV as the excitation energy. The emission spectra were corrected for the spectral response of the emission monochromator and the PM tube.

The photophysical characterization of the spectral relaxation in the pristine polymer is done with a pulsed laser setup consisting of a Spectra Physics Tsunami mode-locked Ti:

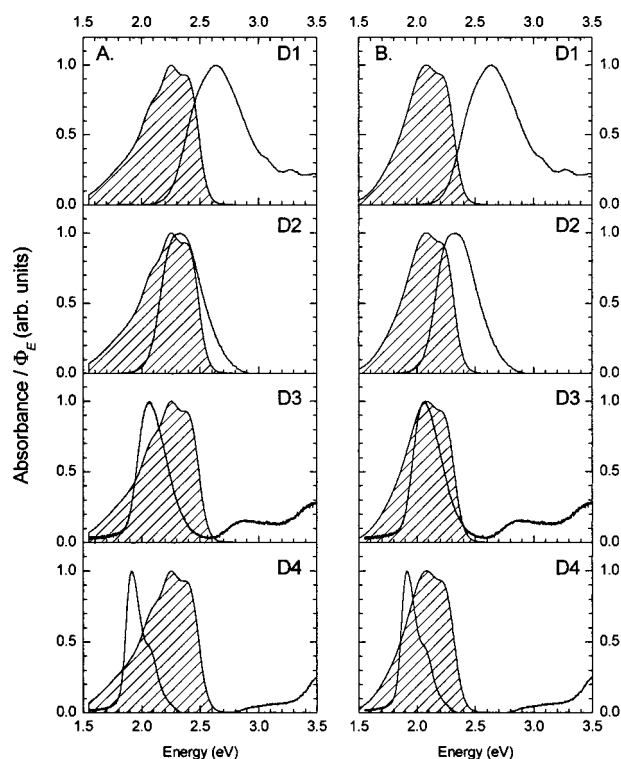


**Figure 2.** (A) Absorption spectra of dyes D1–D4 dispersed in polycarbonate. The hatched area represents the emission band of the pristine green-PPV. (B) Absorption spectra of dyes D1–D4 dispersed in polycarbonate. The hatched area represents the emission band of the pristine yellow-PPV. The emission spectra were obtained upon excitation with 3.0 eV.  $\Phi_E$  denotes the photon flux per constant energy interval.

sapphire laser pumped by a Spectra Physics Millennia Xs pump laser, a Spectra Physics 3980 frequency doubler and pulse selector. Signal detection was carried out with a streak camera (Hamamatsu 5677 slow speed sweep unit) coupled to a Chromex 250is polychromator with a 40 grooves/mm grating. With this setup, a temporal resolution of about 100 ps in a 10 ns detection window is attained. Appropriate filters (Schott) were used to exclude scattered light. Photoexcitation was carried out at 3.5 eV, at a power of several  $\mu\text{W}$  and a spot size of about  $1\text{ mm}^2$ . A typical measurement time was 5–10 min, depending on the sample. The sample was measured while in an airtight container under  $\text{N}_2$  atmosphere and automatically displaced back and forth during the measurement to prevent photooxidation of the polymer. The streak camera images were corrected for the spectral sensitivity of the various optical components and the shading effects due to the deflection plates and the CCD camera by using the streak image and the spectrum of a calibrated blackbody radiator (quartz tungsten halogen lamp).

## Results and Discussion

Dispersions of four different dyes (D1–D4) in two different polymers (green- and yellow-PPV) were prepared and measured. The dye absorption bands overlap the polymer emission bands from the high-energy to the low-energy side (see Figure 2). As a first approach, standard Förster theory can be used to analyze the results.<sup>24,25</sup> This theory is based on dipolar coupling between a donor and an acceptor and gives an expression for the rate constant for energy transfer ( $k_{ET}$ )

$$k_{ET} = \frac{1}{\tau_D} \cdot \left( \frac{R_0}{R} \right)^6 \quad (1)$$

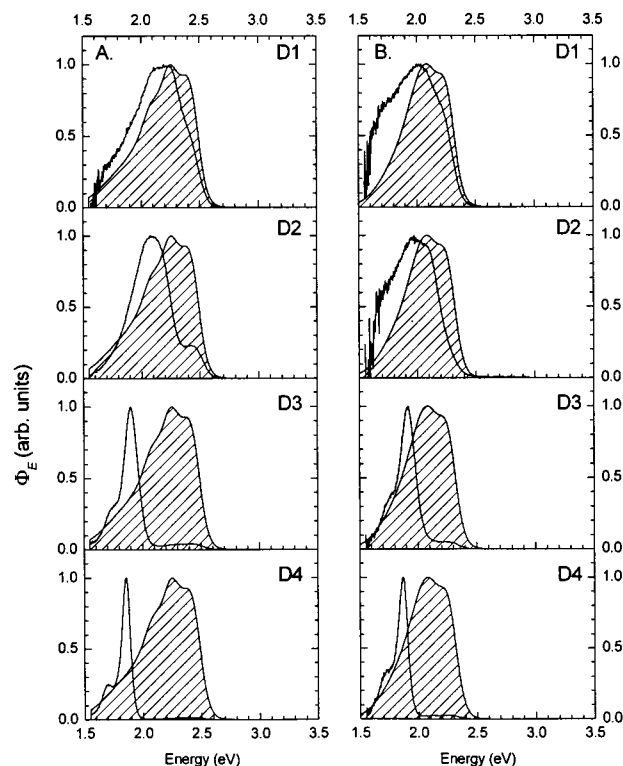


**Figure 3.** (A) Emission spectra of dyes D1–D4 dispersed in green-PPV. The hatched area represents the emission band of the pristine green-PPV. (B) Emission spectra of dyes D1–D4 dispersed in yellow-PPV. The hatched area represents the emission band of the pristine yellow-PPV. The emission spectra were obtained upon excitation with 3.0 eV.  $\Phi_E$  denotes the photon flux per constant energy interval.

**TABLE 1: Spectral Overlap Integrals ( $\Omega$ ) and Förster Radii ( $R_0$ ) of Dye Dispersions in Green- and Yellow-PPV, Respectively.**

dye	$\Omega$ ( $\text{\AA}^6/\text{mol}$ )		$R_0$ ( $\text{\AA}$ )	
	green-PPV	yellow-PPV	green-PPV	yellow-PPV
D1	$9.0 \times 10^{31}$	$2.0 \times 10^{31}$	15	10
D2	$2.0 \times 10^{32}$	$1.3 \times 10^{32}$	17	14
D3	$2.6 \times 10^{32}$	$4.1 \times 10^{32}$	17	17
D4	$1.5 \times 10^{32}$	$3.8 \times 10^{32}$	16	17

which contains the experimental lifetime of the donor emission in the absence of an acceptor ( $\tau_D$ ), the so-called Förster radius ( $R_0$ ), and the donor–acceptor separation ( $R$ ). The Förster radius is a characteristic property of a donor–acceptor system. It depends on the refractive index of the medium ( $n$ ), the relative orientation of the donor and acceptor dipoles ( $\kappa$ ), the quantum yield of the donor emission in the absence of an acceptor ( $Q_D$ ), and the spectral overlap integral (degree of spectral overlap between the donor emission and the acceptor absorption,  $\Omega$ ).

$$R_0^6 = \frac{9000 \ln 10}{128 \pi^5 N_A} \frac{\kappa^2 Q_D}{n^4} \Omega \quad (2)$$

By combining eqs 1 and 2, it is clear that the rate constant for energy transfer is directly proportional to the spectral overlap integral. For the dye dispersions in either green- or yellow-PPV, the values of the spectral overlap integral and the corresponding Förster radii are summarized in Table 1. With respect to the polymer–dye separations ( $R$ ), it was established by confocal microscopy and scanning near-field optical microscopy (SNOM) that each of the dyes was dispersed uniformly in each of the polymers, so that the polymer–dye separations will be similar in all samples.

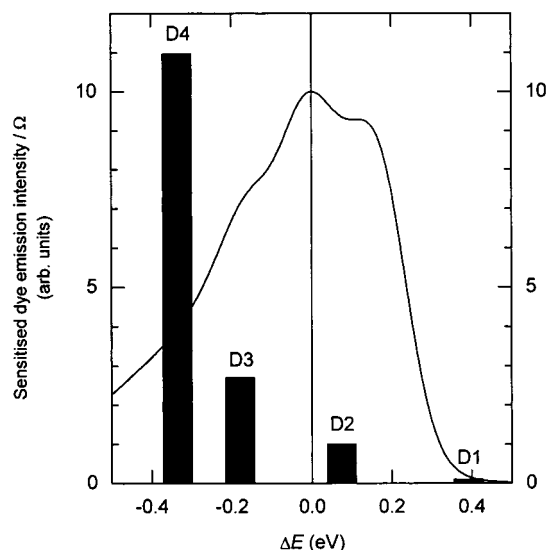


**Figure 4.** Sensitized dye emission intensities corrected for the spectral overlap integral ( $\Omega$ ) for dye dispersions in green-PPV. The sensitized dye emission intensities were determined from the emission spectra after scaling them on the remaining polymer emission. On the abscissa the energy difference between the maxima of the dye absorption band and the polymer emission band ( $\Delta E$ ) are shown. As a reference, the polymer emission spectrum is shown with its maximum at  $\Delta E = 0$ , such that the position of each bar on the abscissa indicates the relative position of the corresponding dye absorption band. Note: although a dispersion of D1 in green-PPV does not show significant energy transfer (i.e., the bar should have zero length), a small bar is nevertheless shown to indicate the relative energetic position of the D1 absorption band.

Figure 3 contains the emission spectra of the polymer-dye combinations. In both green- and yellow-PPV the four dyes show markedly different sensitized emission intensities. First of all, steady-state measurements on dispersions of D1 in both green- and yellow-PPV and of D2 in yellow-PPV do not show efficient energy transfer. With respect to the other dye dispersions (D2-D4 in green-PPV and D3-D4 in yellow-PPV), the relative intensities of the sensitized dye emissions can be measured by making use of the fact that in all these samples still some remaining polymer emission is present (meaning that for neither of these combinations the energy transfer is 100% efficient). First, the emission spectra are scaled on the remaining polymer emission, after which the integrated intensity of the sensitized dye emission can be determined. These intensities can subsequently be corrected for the values of the spectral overlap integral. As the rate constant for energy transfer depends linearly on the spectral overlap integral, it is necessary to correct for this before comparing the different dye dispersions, although the Förster radii of these dispersions are comparable (see Table 1).

For dye dispersions in green-PPV, Figure 4 contains the results of this procedure plotted versus the energy difference between the maxima of the dye absorption band and the polymer emission band (which indicates the spectral position of the dye absorption with respect to the polymer emission). The trend shown in Figure 4 cannot result from differences in quantum efficiencies of the dyes, as the quantum efficiencies of all dyes lie between 0.7 and 0.9 in green- and yellow-PPV. From Figure 4 it is clear that when the maximum of the dye absorption band is positioned more to the low-energy part of the green-PPV emission band, the sensitized dye emission intensity corrected for the spectral overlap integral increases strongly. This series of dye dispersions was prepared and measured several times, and always the same clear trend was observed. For dye

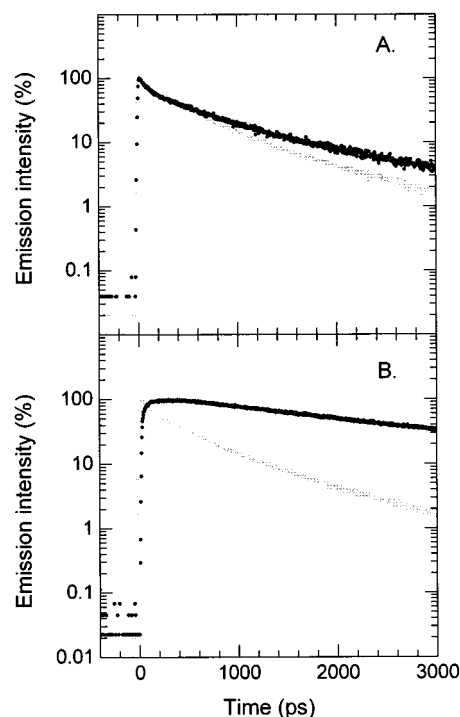


**Figure 5.** (A) The luminescence decays of pristine green-PPV (grey, emission monitored at 2.40 eV with a detection window of 0.04 eV), and of green-PPV doped with D2 (black, emission monitored at 2.13 eV with a detection window of 0.03 eV). (B) The luminescence decays of pristine green-PPV (grey, emission monitored at 2.40 eV with a detection window of 0.04 eV), and of the green-PPV doped with D4 (black, emission monitored at 1.86 eV with a detection window of 0.03 eV).

dispersions in yellow-PPV a similar trend is found, although in this case it is less straightforward to scale the emission spectra on the remaining polymer emission. Obviously, in dye-doped polymers the energy transfer efficiency is not only determined by energetic resonance between the polymer and the dye (spectral overlap integral) and by the separation between the polymer and the dye, but also the energetic position of the dye absorption band with respect to the polymer emission band is of great importance.<sup>26</sup>

To study the temporal behavior of the photoluminescence of dye-doped polymers, time-correlated single photon counting (TCSPC) measurements were performed. Only a selection of these TCSPC measurements, which represent the typical decay patterns found for the dye-doped polymers, will be presented here. Those cases for which energy transfer occurs can be discussed using one of two examples mentioned below.

The first example is formed by those dyes whose absorption band overlaps the high energy side of the polymer emission band (e.g., D2 in green-PPV). From Figure 4 it is clear that green-PPV doped with D2 does not show efficient energy transfer. Figure 5A shows the luminescence decays of pristine green-PPV (monitored at 2.40 eV, the maximum of the polymer emission, with a detection window of 0.04 eV) and of a dispersion of D2 in green-PPV (monitored at 2.13 eV, the maximum of the D2 emission, with a detection window of 0.03 eV). Although energy transfer is observed in steady-state measurements, the typical signature of energy transfer in time-resolved measurements—a rise time of the emission originating from the dye<sup>27</sup>—is absent. Apparently the rise time of the dye emission is masked by the strong polymer emission on this short time scale, which also renders the overall energy transfer inefficient. For this case, the temporal profile of the emission



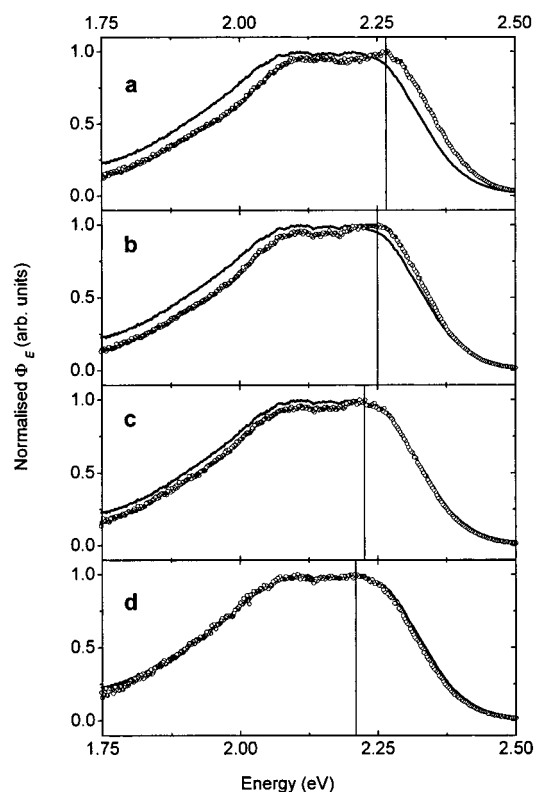


**Figure 6.** Emission spectra of yellow-PPV as measured in 200 ps time windows, using a streak camera. The black line in (a)–(d) represents the time integrated (steady state) emission spectrum and the open circles depict the emission spectra in the time windows (a) 0–200 ps, (b) 200–400 ps, (c) 500–700 ps, and (d) 1–1.2 ns.

from the dispersed dye can be roughly divided in two phases. In the first phase, the emission decay is fast and identical to that of the pristine polymer, while in the second phase the emission decay is much slower and characteristic of the dye.

The second example is formed by dyes whose absorption band overlaps the low energy side of the polymer emission band (e.g., D4 in green-PPV). From the steady-state luminescence spectrum (see Figure 3) and Figure 4 it is clear that green-PPV doped with D4 shows quite efficient energy transfer. Figure 5B shows the luminescence decays of pristine green-PPV (monitored at 2.4 eV, the maximum of the polymer emission, with a detection window of 0.04 eV) and of a dispersion of D4 in green-PPV (monitored at 1.86 eV, the maximum of the D4 emission, with a detection window of 0.03 eV). For this polymer–dye system, a rise time in the temporal profile of the dye emission is clearly visible. The decay profile of the doped polymer does not follow the kinetics of the pristine polymer.

These two examples clearly illustrate that the energetic position of the dye absorption band within the profile of the polymer emission band (not to be confused with the spectral overlap integral!) is very important. The temporal behavior of the polymer emission provides more insight into this phenomenon. In Figure 6, the evolution of the polymer emission spectrum as a function of time is shown and compared to the time-integrated emission spectrum. The time-resolved spectra in Figure 6a–d (open circles) represent integrations of the polymer emission band in 200 ps time windows at (a) 0–200 ps, (b) 200–400 ps, (c) 500–700 ps, and (c) 1–1.2 ns, respectively. It can be seen that over time the polymer emission spectrum shifts to lower energy. This spectral red shift can take place on time scales of several ps to several ns, depending on the nature of the polymer.<sup>18,28</sup> Regardless of the nature of this

temporal spectral shift, dyes in disordered polymers interact with time-variant spectral energy distributions. The steady-state emission spectrum, which is included in the spectral overlap integral, is a convolution of time-dependent emission spectra. This limits the use of the spectral overlap integral in describing time-dependent processes such as excited-state energy transfer.

Such dynamic Stokes shifts as seen above have been related to energy dispersive exciton relaxation in an inhomogeneously broadened distribution of states<sup>18,19,29</sup> and more recently to structural relaxation mechanisms,<sup>30</sup> the extent to which of the two is relevant depending on structural features of the polymers examined. We see the observations described above in a variety of polymers, some of which are especially designed to minimize intermolecular chain interaction in order to increase the quantum yield and prevent color point shifting for usage as emissive layers in LEDs (e.g., random copolymers such as yellow-PPV shown in Figure 6). Thermal treatment of these sort of polymers in an inert atmosphere does not result in a spectral change or in sharp peaks in the X-ray diffraction pattern. We do observe such effects in, for example, OC<sub>1</sub>C<sub>10</sub>–PPV or some fluorene-type polymers, which we therefore did not use in our investigation. Consequently we anticipate that the relaxation mechanism in green- and yellow-PPV is more likely to be excitonic relaxation in an inhomogeneously broadened distribution of states than due to interchain packing interactions.

To discuss the results as mentioned above, one has to start by looking at the polymer only and describe the processes following excitation of the polymer. First of all, one can think of a disordered polymer chain as consisting of conformational segments separated by kinks. Especially for  $\pi$ -conjugated disordered polymers, the question arises whether the instantaneous optical polarization by a coherent source (in our case a fs laser) is either quasi localized on a few segments or delocalized over a large number of segments.<sup>31</sup> The structural disorder results in a broad range of intersegmental interaction strengths ranging from only slightly perturbing the conjugation to totally disrupting it. As a consequence, the initial excitation is of largely intersegmental delocalized character on strongly coupling segments and of more localized character on weakly coupling segments. The excitation energy on these differently coupled segments can dephase according to different mechanisms, which leads to uncorrelated exciton populations at times longer than the coherence time. On the time scale of our experiments (TCSPC  $\sim$ 20 ps fwhm of the instrument response function), one is dealing with such uncorrelated exciton populations, and the relaxation of the exciton population can be described by energy dispersive excitation transfer.<sup>32,33,19</sup>

Due to the dispersive transfer of excitons, the photons constituting the high-energy side of a polymer emission band originate from states in the polymer from which excitons can migrate at a much higher rate than from low-energy states. Concerning the nature of the low-energy states (from which no or hardly any dispersive exciton transport occurs), they could either belong to the longest conjugated parts of a disordered polymer chain, to dimers, or to aggregates. Whatever the exact nature of these states may be, the important point for our discussion is that exciton lifetime increases when the excitons migrate to progressively lower energy states of the polymer, due to the absence of suitable interaction partners at lower energies.<sup>26</sup>

The results described above show that standard Förster theory, describing *one* energy transfer process involving *one* donor and *one* acceptor, is not adequate to describe the observed energy transfer behavior in doped polymers. Instead, one should realize

that in doped polymers the donor is in fact an ensemble of donors leading to the existence of donor-donor energy transfer in addition to donor-acceptor energy transfer. The kinetic balance within such a superposition of energy transfer processes determines the efficiency of donor-acceptor (in this case, polymer-dopant) energy transfer.

To illustrate the excitation energy transfer processes in such complex systems, two processes that are competing with each other can be considered: (1) dispersive transport of excitons within a disordered polymer and (2) transfer of excitons from a polymer to a dye molecule. The rate constants for these two processes can be written as

$$k_1 \equiv \frac{1}{\tau_1} \wedge k_2 = \frac{1}{\tau_2} \cdot \left(\frac{R_0}{\bar{R}}\right)^6 \quad (3)$$

Here,  $\bar{R}$  is the mean distance over which the exciton has to be transferred from polymer to dye, and  $\tau_2$  is the lifetime of the polymer in the absence of a dye.

While polymer-to-dye energy transfer can be described by Förster theory, this is less straightforward for dispersive exciton transport within the polymer. For this process, the dipolar approximation probably does not hold in a short time range following the creation of excitons.

Physically, the characteristic time  $\tau_1$  can be described as the time it takes an exciton to jump from site  $i$  to site  $j$  within the disordered polymer. Another way of putting this is to say that  $\tau_1$  is the lifetime of the exciton in site  $i$ , which is called the *dwelt time*.<sup>26</sup> As mentioned before, in a disordered polymer the dwelt time is shortest at the high-energy side of the energetic distribution of states, and gradually increases toward the low energy side of this distribution.

For a dye dispersion in a disordered polymer, polymer-to-dye energy transfer is more efficient than intrapolymer exciton migration when  $k_2 > k_1$ , which can be written as

$$\frac{\bar{R}}{R_0} < \left(\frac{\tau_1}{\tau_2}\right)^{1/6} \quad (4)$$

The lifetime ratio on the right-hand side of eq 4 is not constant but is different for each site in the disordered polymer. This ratio has a maximum of unity as the dwelt time cannot exceed the lifetime of the polymer emission. Each dye dispersion in a disordered polymer is characterized by a specific value for the ratio  $\bar{R}/R_0$ . An exciton can only be transferred efficiently from a certain site in the disordered polymer to a dye when the lifetime ratio ( $\tau_1/\tau_2$ ) of this site is larger than the characteristic ratio  $\bar{R}/R_0$  to the sixth power. Equation 4 is visualized graphically in Figure 7. From this graph it is clear that when the dwelt time becomes shorter than the lifetime of the polymer emission (lifetime ratio becomes smaller than unity), the maximum ratio  $\bar{R}/R_0$  initially does not decrease very strongly. Only for those sites whose dwelt time is very short compared to the lifetime of the polymer emission does the ratio  $\bar{R}/R_0$  decrease rapidly, indicating that excitons in such sites can be transferred efficiently to a dye only when the distance from that site to the dye is very short or when the Förster radius is very large.

A value for  $\tau_2$  can be obtained from time-resolved emission measurements on a pristine polymer,  $\tau_2$  being the lifetime of this emission at a certain energy (typically 1–1.5 ns at the low-energy side of the polymer emission band). From the same type of measurements, looking at the rise time of the polymer emission at a certain energy, values for the dwelt times ( $\tau_1$ ) can be extracted (it has been shown that at the high-energy side

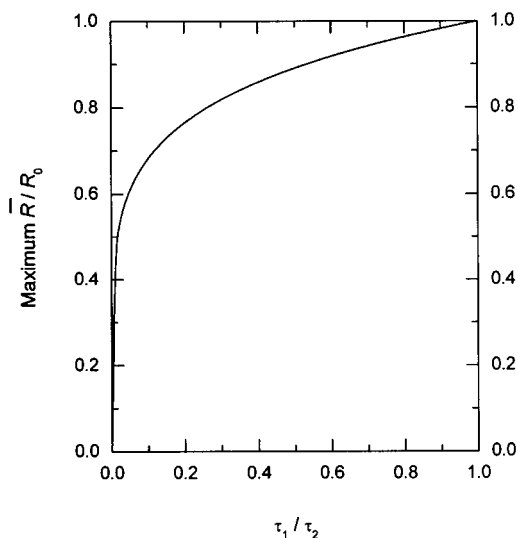


**Figure 7.** Graphical representation of eq 4. The abscissa contains the ratio of the dwell time ( $\tau_1$ ) to the lifetime of the polymer emission ( $\tau_2$ ), for a certain polymer excited-state energy. The ordinate gives the maximum mean relative polymer-dye distance ( $\bar{R}/R_0$ ) that a polymer-dye combination should have for the particular excited state energy to be transferred efficiently from the polymer to the dye.

of the polymer emission band the dwell time is approximately 300 fs).<sup>34</sup> Since the dwell time increases during the downhill relaxation of excitons through the density of states, it will eventually become equal to the polymer-to-dye energy transfer time and from that point on the latter process will take over to dominate (it is assumed that the polymer-to-dye energy transfer time is constant). In this line of argumentation, a dye that has its highest absorption strength at the same energy as where the polymeric sites (the longest conjugated parts of a disordered polymer chain, dimers, or aggregates) have dwell times longer than the polymer-to-dye energy transfer time should exhibit efficient energy transfer. The dyes D3 and D4 fulfill this condition and, as can readily be seen in the steady-state spectra and the time-resolved measurements, very efficient energy transfer takes place in all polymers used here. Due to the relatively low polymer emission intensity at the maximum of the dye emission, the rise time of the dye emission is visible and not blurred by emission originating from the polymer.

Due to the stochasticity of photoluminescence, emission will originate to some degree from the polymeric states at the high-energy side of the density of states distribution. A dye dispersion in a disordered polymer will therefore have a residual polymer emission with less intensity at the low-energy side as compared to the emission from the pristine polymer (see Figure 8).

Concerning the polymer-dye systems described in this article, three possible situations can be distinguished with respect to the spectral position of the dye absorption band relative to the polymer emission band. The first situation is when the maximum of the dye absorption band is located at the high-energy side of the time-integrated polymer emission band (D1 in both green-PPV and yellow-PPV and D2 in yellow-PPV). The only excitons that are energetically resonant with the dye are subject to a very fast dispersive transfer within the polymer itself. Transfer of these excitons from the polymer to the dye will therefore be very inefficient. As a result, the emission spectrum resembles that of the pristine polymer (see Figure 3), only with slightly less intensity at the high-energy side of the emission band. A second situation is when the maximum of the dye absorption band overlaps with the maximum of the time-integrated polymer emission band (D2 in green-PPV and D3 in yellow-PPV). The

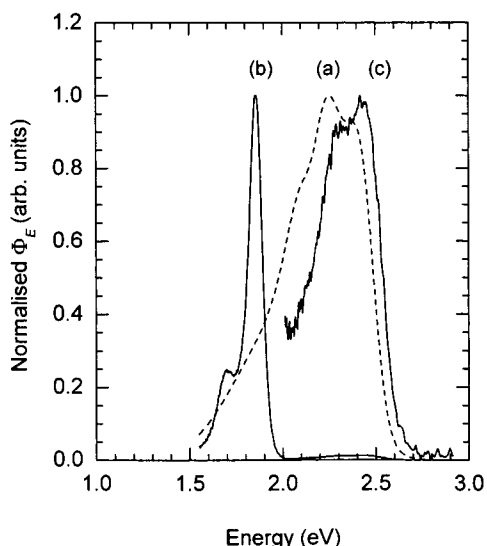


**Figure 8.** Emission spectrum of pristine green-PPV (a) and of green-PPV doped with dye D4 at a mass ratio of 0.75% (b). An enlargement of the part of spectrum (b) that shows the remaining polymer emission is shown as (c). The emission spectra were obtained upon excitation with 3.0 eV.  $\Phi_E$  denotes the photon flux per constant energy interval.

energetically resonant excitons are now less mobile than in the previous situation and can be transferred to the dye more efficiently. The emission spectrum shows relatively strong dye emission but also still a considerable polymer rest emission (see Figure 3). The third situation is when the maximum of the dye absorption is located at the low-energy side of the time-integrated polymer emission band (D3 in green-PPV and D4 in both green-PPV and yellow-PPV). The energetically resonant excitons can be transferred efficiently from the polymer to the dye as they have almost completely relaxed within the polymer density of states distribution. Nevertheless, a small amount of polymer emission still remains, originating from states that are not resonant with states of the dye (see Figure 3).

The occurrence of residual polymer emission is of particular practical importance if the polymer itself emits green light while the dye emits red light. Due to the variable color sensitivity of the human eye, any spurious green emission in a predominantly red emitting device leads to an orange color perception.<sup>35</sup> As will be shown next, this finding has implications for the use of doped polymers as emitting layers in polymer light-emitting devices (PLEDs). When the excitons are created on the polymer and have to be transferred to dye molecules that are dispersed in this polymer, some polymer emission will always remain. Figure 9 illustrates this effect for D4 at different concentrations in yellow-PPV. The relative contributions of the polymer emission (open circles) and dye emission (solid circles) to the total emission intensity in both electroluminescence (solid line) and photoluminescence (dashed line) is plotted as a function of the dye-to-polymer mass ratio. It can be seen that the trend is the same for both photoluminescence and electroluminescence and for all dye-to-polymer mass ratios a polymer rest emission is present. While in photoluminescence the dye can only be excited via energy transfer (provided that only the polymer is photoexcited), in electroluminescence the dye can also be excited via trapping of charge carriers. This can be seen in Figure 9 as the contribution of the dye emission to the total emission is larger in electroluminescence than in photoluminescence, indicating the presence of an extra mechanism to excite the dye molecules in electroluminescence. The fact that in electroluminescence residual polymer emission is also present indicates

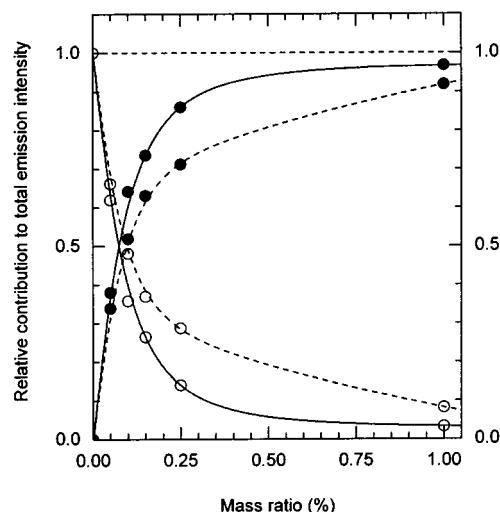


**Figure 9.** Relative contribution to the total emission intensity in photoluminescence (dashed line) and electroluminescence (solid line) of the polymer emission (open circles) and the dye emission (solid circles), for dispersions of dye D4 in yellow-PPV, as a function of dye-to-polymer mass ratio.

that still a number of excitons is created on the polymer. For use in devices this means that dye molecules are not solely excited via trapping of charge carriers on the dye but also, to some degree, via energy transfer from the polymer.

Figure 9 indicates that the unwanted residual polymer emission can be largely suppressed by increasing the dye-to-polymer mass ratio to such an extent that the polymer-to-dye transfer rate exceeds the intrapolymer relaxation rate. However, from a certain dye-to-polymer mass ratio (0.75% in our case) concentration quenching and aggregation starts to play a prominent role and the absolute dye emission intensity decreases considerably. A possible way to avoid aggregation at high dye-to-polymer mass ratios is to chemically attach the dye to the polymer chain. This approach will also lead to higher energy transfer efficiencies, which would suppress the residual polymer emission even further. Another approach that prevents residual polymer emission is to use the polymer only as a medium to transfer charge carriers from the electrodes to the dye molecules where they can recombine and emit. Future work will be dedicated toward exploring these approaches for polymer light-emitting devices.

## Conclusion

It is shown that efficient excitation energy transfer from a disordered polymer showing dispersive exciton transport to a dopant is not just a matter of energetic resonance between polymer and dopant but strongly depends on the ratio of the intrapolymer exciton migration rate and the polymer-to-dopant energy transfer rate, particularly at the energy at which the dopant has its maximum absorption. Consequently, dye-doped polymers that are optimized only for the spectral overlap integral will not necessarily exhibit optimal energy transfer characteristics resulting in the presence of residual polymer emission. Although in electroluminescent devices trapping of charge carriers by dye molecules operates as an additional mechanism to excite dye molecules, resulting in a relatively stronger dye emission as compared to that in photoluminescence, in devices comprising the polymer-dye systems described here, transfer of excitons from polymer to dye also occurs. Therefore, these electroluminescent devices also show residual polymer emission. It is of particular practical importance that this residual polymer

emission is suppressed as, for example, any spurious green emission in a predominantly red emitting device leads to an orange color perception, due to the variable color sensitivity of the human eye.

**Acknowledgment.** The authors gratefully acknowledge Prof. Dr. M. Glasbeek and D. Bebelaar from the University of Amsterdam for using their TCSPC equipment, and Marijn Goes (University of Amsterdam) for helping with the measurements. Dr. S. de Feyter from the Katholieke Universiteit Leuven (Belgium) is acknowledged for performing the confocal microscopy and scanning near-field optical microscopy measurements on the dye-doped polymers.

## References and Notes

- (1) Burroughes, J. H.; Bradley, D. D. C.; Brown, A. R.; Marks, R. N.; Mackay, K.; Friend, R. H.; Burns, P. L.; Holmes, A. B. *Nature* **1990**, *347*, 539.
- (2) Morgado, J.; Cacialli, F.; Friend, R. H.; Iqbal, R.; Yahioglu, G.; Milgrom, L. R.; Moratti, S. C.; Holmes, A. B. *Chem. Phys. Lett.* **2000**, *325*, 552.
- (3) Haring Bolivar, P.; Wegmann, C.; Kersting, R.; Deussen, M.; Lemmer, U.; Mahrt, R. F.; Bässler, H.; Göbel, E. O.; Kurz, H. *Chem. Phys. Lett.* **1995**, *245*, 534.
- (4) Kido, J.; Shionoya, H.; Nagai, K. *Appl. Phys. Lett.* **1995**, *67*, 2281.
- (5) Lemmer, U.; Ochse, A.; Deussen, M.; Mahrt, R. F.; Göbel, E. O.; Bässler, H.; Haring Bolivar, P.; Wegmann, C.; Kurz, H. *Synth. Met.* **1996**, *78*, 289.
- (6) Brütting, W.; Berleb, S.; Egerer, G.; Schwoerer, M.; Wehrmann, R.; Elschner, A. *Synth. Met.* **1997**, *91*, 325.
- (7) Jang, M. S.; Song, S. Y.; Shim, H. K.; Zyung, T.; Jung, S. D.; Do, L. M. *Synth. Met.* **1997**, *91*, 317.
- (8) Hu, B.; Zhang, N.; Karasz, F. E. *J. Appl. Phys.* **1998**, *83*, 6002.
- (9) Shoustikov, A. A.; You, Y.; Thompson, M. E. *IEEE J. Sel. Top. Quantum Electron.* **1998**, *4*, 3.
- (10) Dicker, G.; Hohenau, A.; Graupner, W.; Tasch, S.; Graupner, M.; Hermetter, A.; Schlicke, B.; Schulte, N.; Schlüter, A. D.; Scherf, U.; Müllen, K.; Leising, G. *Synth. Met.* **1999**, *102*, 873.
- (11) List, E. J. W.; Creely, C.; Leising, G.; Schulte, N.; Schlüter, A. D.; Scherf, U.; Müllen, K.; Graupner, W. *Chem. Phys. Lett.* **2000**, *325*, 132.
- (12) Virgili, T.; Lidzey, D. G.; Bradley, D. D. C. *Adv. Mater.* **2000**, *12*, 58.
- (13) Rauscher, U.; Schütz, L.; Greiner, A.; Bässler, H. *J. Phys. Condens. Matter* **1989**, *1*, 9751.
- (14) Kersting, R.; Mollay, B.; Rusch, M.; Wenisch, J.; Leising, G.; Kauffmann, H. F. *J. Chem. Phys.* **1997**, *106*, 2850.
- (15) Haan, S. W.; Zwanzig, R. J. *J. Chem. Phys.* **1978**, *68*, 1879.
- (16) Rauscher, U.; Bässler, H.; Bradley, D. D. C.; Hennecke, M. *Phys. Rev. B* **1990**, *42*, 9830.
- (17) Heun, S.; Mahrt, R. F.; Greiner, A.; Lemmer, U.; Bässler, H.; Halliday, D. A.; Bradley, D. D. C.; Burn, P. L.; Holmes, A. B. *J. Phys. Condens. Matter* **1993**, *5*, 247.
- (18) Kersting, R.; Lemmer, U.; Mahrt, R. F.; Leo, K.; Kurz, H.; Bässler, H.; Göbel, E. O. *Phys. Rev. Lett.* **1993**, *70*, 3820.
- (19) Meskers, S. C. J.; Hübner, J.; Oestreich, M.; Bässler, H. *Chem. Phys. Lett.* **2001**, *339*, 223.
- (20) Visser, R. J. *Philips J. Res.* **1998**, *51*, 467.
- (21) Gilch, H. G.; Wheelwright, W. L. *J. Polym. Sci., Part A: Polymer Chem.* **1966**, *4*, 1337.
- (22) Becker, H.; Spreitzer, H.; Kreuder, W.; Kluge, E.; Schenk, H.; Parker, I. D.; Cao, Y. *Adv. Mater.* **2000**, *12*, 42.
- (23) van Dijk, S. I.; Wiering, P. G.; Groen, C. P.; Brouwer, A. M.; Verhoeven, J. W.; Schuddeboom, W.; Warman, J. M. *J. Chem. Soc., Faraday Trans.* **1995**, *91*, 2107.
- (24) Förster, T. *Ann. Phys.* **1948**, *2*, 55.
- (25) Lakowicz, J. R. *Principles of Fluorescence Spectroscopy*, 2nd ed.; Kluwer Academic/Plenum Publishers: New York, 1999.
- (26) Mollay, B.; Lemmer, U.; Kersting, R.; Mahrt, R. F.; Kurz, H.; Kauffmann, H. F.; Bässler, H. *Phys. Rev. B* **1994**, *50*, 10769.
- (27) O'Connor, D. V.; Phillips, D. *Time-correlated single photon counting*; Academic Press: London, 1984.
- (28) Brunner, K.; Tortschanoff, A.; Warmuth, C.; Bässler, H.; Kauffmann, H. F. *J. Phys. Chem. B* **2000**, *104*, 3781.
- (29) Kennedy, S. P.; Garro, N.; Phillips, R. T. *Phys. Rev. B* **2001**, *64*, 115206.
- (30) Bjorklund, T. G.; Lim, S. H.; Bardeen, C. J. *J. Phys. Chem. B* **2001**, *105*, 11970.
- (31) Sperling, J.; Milota, F.; Tortschanoff, A.; Warmuth, C.; Kauffmann, H. F. In *Femtochemistry and Femtobiology. Ultrafast dynamics in molecular science*; Douhal, A., Santamaria, J., Eds.; Proceedings of the Vth Femtochemistry Conference (Toledo, Spain 2001); World Scientific Publishing House: Singapore, in press.
- (32) Byers, J. D.; Parsons, W. S.; Friesner, R. A.; Webber, S. E. *Macromolecules* **1990**, *23*, 4835.
- (33) Kauffmann, H. F.; Mollay, B. Dynamics of energy transfer in aromatic polymers. In *Disorder effects on relaxational processes*; Richert, R., Blumen, A., Eds.; Springer-Verlag: Berlin, 1994.
- (34) Brunner, K.; Tortschanoff, A.; Warmuth, C.; Mollay, B.; Kauffmann, H. F. *Phys. Status Solidi B* **1998**, *205*, 325.
- (35) Bouma, P. J. *Physical Aspects of Colour; An Introduction to the Scientific Study of Colour Stimuli and Colour Sensations*; Philips Technical Library: Eindhoven, 1971.